Compact Fully Integrated Rectenna System with a Reconfigurable Power Management System for Energy Harvesting at 2.45 GHz

Jelle Jocqué, Joryan Sennesael, Jo Verhaevert, Patrick Van Torre, and Hendrik Rogier
Department of Information Technology (INTEC), IDLAB, Ghent-University-imec, Ghent, Belgium

***Abstract*—This paper presents a fully integrated and compact rectenna system designed for radio frequency energy harvesting at 2.45 GHz, aimed at powering low-power applications such as semi-passive and active radio frequency identification systems. The rectenna system co-optimizes the antenna and rectifier, eliminating the need for an impedance matching network, thereby reducing transfer losses and its size. A reconfigurable central power management system and a supercapacitor are incorporated, featuring maximum power point tracking, enabling efficient power harvesting and delivery. The antenna design is based on a meandered-line planar inverted-F antenna, which provides compactness, ease of integration on a low-cost FR4 substrate, and an omnidirectional radiation pattern. Over-the-air power conversion efficiency measurements were conducted, demonstrating high efficiency at low input power levels, ranging from -13 dBm to -1 dBm. The system's functionality was further validated by powering a wireless body temperature sensor application, featuring a packet update rate of 14m24s for an input power level of -10 dBm.**

***Index Terms*—Rectenna, Energy Harvesting, Power Management System, Supercapacitor**

I. Introduction

Radio frequency (RF) energy harvesting (EH) and other wireless power transfer (WPT) technologies have gained significant attention owing to their potential to advance wireless applications and enhance the efficiency of radio frequency identification (RFID) systems [1]. Specifically, these technologies offer a promising solution to extend the operational lifetime and autonomy of semi-passive and active RFID, which have traditionally relied on batteries or external power sources. This dependency restricts their operational lifespan and increases maintenance efforts, especially in remote or inaccessible locations. By capturing ambient RF energy from sources such as Wi-Fi, cellular networks or dedicated RF transmitters, EH enables RFID tags to power their circuits, thereby reducing their dependence on batteries or facilitating battery-less designs.

To effectively harness WPT, the design and optimization of rectenna systems are crucial. These systems must be co-optimized to ensure efficient power transfer between the antenna, rectifier, and central power management system (CPMS), while minimizing losses and maximizing efficiency [2]. For widespread adoption, rectenna systems must be compact, cost-effective, and easily integrable into both existing and next-generation RFID applications without sacrificing performance. A well-designed CPMS incorporating maximum power point tracking (MPPT) is essential for maximizing the power harvested by the rectifier.

In [3], a full rectenna system is presented for battery charging through RF EH at 2.45 GHz. The system can source 5.8 µJ at -20 dBm RF input power in one hour, but has a large size of 100 mm by 100 mm. In [4], an energy-autonomous simultaneous wireless information and power transfer (SWIPT) RFID Tag with a lumped-components rectifier at 915 MHz and an integrated CPMS is proposed. Tests on the system showed that with a minimum input power of -20 dBm, it was possible to sustain the energy requirements of a transceiver for an active state framed by TX/RX cycles.

In this paper, we propose a highly compact, fully integrated rectenna system for EH at 2.45 GHz. The antenna is co-designed and co-optimized with the rectifier, thereby eliminating the impedance matching network, reducing transfer losses and increasing efficiency. Additionally, a CPMS is integrated into the rectenna system, offering reconfigurability based on the required output voltage and the total energy demand of the application.

II. Rectenna System

This section presents the proposed fully integrated rectenna system, comprising three main components: the antenna, the rectifier, and the CPMS. First, the design of the rectifier is briefly discussed, followed by an overview the design of the antenna, which is directly matched to the input impedance of the rectifier. The output of the rectifier is connected to the input of the CPMS, which includes a highly efficient energy management circuit with minimal external components, and a supercapacitor as the energy storage element. Measurement results detailing the performance of the rectenna system are presented. Finally, a practical application example is discussed, demonstrating how the rectenna can be used to power an actual device and how the system can be configured using just a few resistors.

A. Rectifier Design

The rectifier used in this rectenna design was previously published in [**?**] and is based on the SMS7630-005LF series pair Schottky diodes in a SOT-23 package [5]. Typically, a matching network is employed to optimize power transfer between the antenna and rectifier. However, in this design, the antenna's input impedance is conjugate-matched directly to the input impedance of the rectifier, reducing the PCB footprint and minimizing transfer losses. The rectifier's input impedance varies with both load impedance and input power. Since the rectifier's power conversion efficiency (PCE) was optimized for a load impedance of 4.7 kΩ in [**?**], this contribution focuses solely on the influence of input power.

To simulate the input impedance of the rectifier at various input power levels, it is necessary to determine the voltage level at the junction between the cathode of the first diode and the anode of the second diode (shown in Fig. 1) as a function of input power. For input power levels of -13 dBm, -7 dBm, -3 dBm and 0 dBm, the simulated voltage levels are 114 mV, 280 mV, 481 mV and 705 mV, respectively. The co-design process begins at an input power level of -13 dBm because the CPMS requires an input power of -19 dBm to initiate a cold start. Achieving this requires the rectenna to operate with a minimum PCE of 25 % at an input power level of -13 dBm. Next, the input impedance of the voltage doubler can be determined over the frequency range of 2.35 GHz to 2.55 GHz, as shown in Fig. 1. It is observed that the real part of the input impedance of the rectifier increases with rising input power while the reactance remains relatively constant.

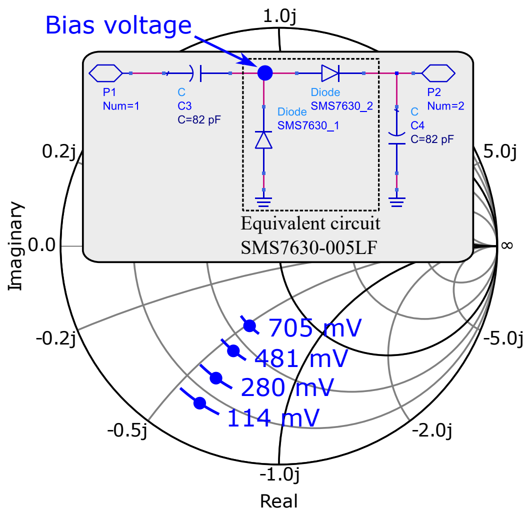

Fig. 1: Smith diagram with normalized input impedance (port P1) from 2.35 to 2.55 GHz of the rectifier with a load impedance of 4.7 kΩ (port P2) for a bias voltage of 114 mV, 280 mV, 481 mV and 705 mV.

B. Antenna Design

The chosen antenna topology for this rectenna design is a meandered-line planar inverted-F antenna (PIFA) owing to its compact size, ease of integration on a low-cost FR4 substrate, and its omnidirectional radiation pattern. The antenna is designed and manufactured on an IS400 substrate, which has a dielectric constant ϵ_r of 3.9 and a loss tangent $tan(\delta)$ of 0.022. A two-layer design is employed, with a substrate thickness of 1.55 mm and a metal layer thickness of 35 µm. All relevant antenna dimensions are provided in Fig. 2.

The antenna design and optimization process are carried out in two stages. First, the radiation efficiency and radiation pattern are optimized based on a 50 Ω reference impedance at a target frequency of 2.45 GHz. Second, the input impedance of the antenna is conjugate-matched to the rectifier's input

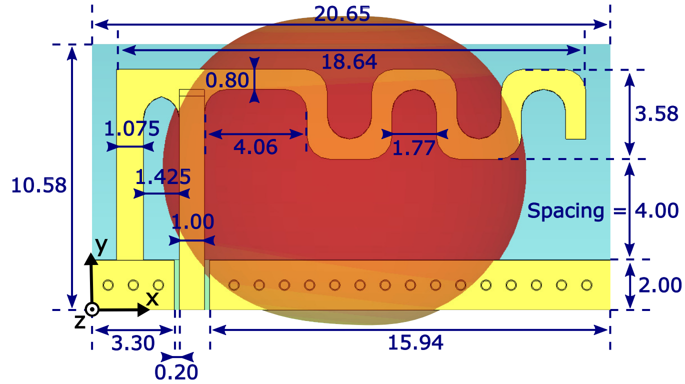

Fig. 2: Dimensions in mm and 3D radiation pattern of the designed meandered-line PIFA (copper in yellow and IS400 substrate in blue).

impedance for an input power range from -13 dBm to -2 dBm, which are typical levels for far-field WPT applications. For the conjugate-matching process, the S-parameters of the rectifier without a matching network were exported into the antenna simulation environment using CST Microwave Studio (MWS). By leveraging the post-processing tools within CST MWS, S-parameter tasks were defined, allowing the imported rectifier S-parameters to be used in optimizing the matching between the antenna and rectifier. This approach ensured efficient co-design, minimizing impedance mismatches and enhancing overall system performance. In this design, the key parameter for adjusting the antenna's input impedance to match the rectifier's input impedance is the spacing between the folded dipole and the ground plane. Modifying this spacing directly affects the real part of the input impedance, with minimal impact on the reactance, as illustrated in Fig. 3. This approach allows for efficient co-optimization of the antenna and rectifier circuit without altering the operating frequency or the far-field radiation pattern.

In Fig. 4, the magnitude of the reflection coefficient $|S_{11}|$ is plotted in dB for four different input power levels: -13 dBm, -7 dBm, -3 dBm and 0 dBm. It can be observed that the rectifier achieves a reflection coefficient below -10 dBm at a frequency of 2.45 GHz for input power levels: -13 dBm, -7 dBm and -3 dBm, with optimal matching occurring at -7 dBm. The antenna exhibits an omnidirectional radiation pattern with a maximum gain of 0.43 dBi and a radiation efficiency of 78 %, as shown in Fig. 2.

C. Power Management System Design

The rectenna system includes a fully operational CPMS based on the AEM30940 energy management circuit from E-Peas [6]. The AEM30940 features a cold start input power of -19 dBm, which requires a minimum input power of -13 dBm to function effectively, along with a PCE of 25 %, as discussed in II-A. The MPPT is configured to an optimal ratio of 50 % between the maximum power point (MPP) voltage and the open-circuit voltage. This ratio was determined after evaluating the rectifier's measured and simulated I-V and P-V characteristics.

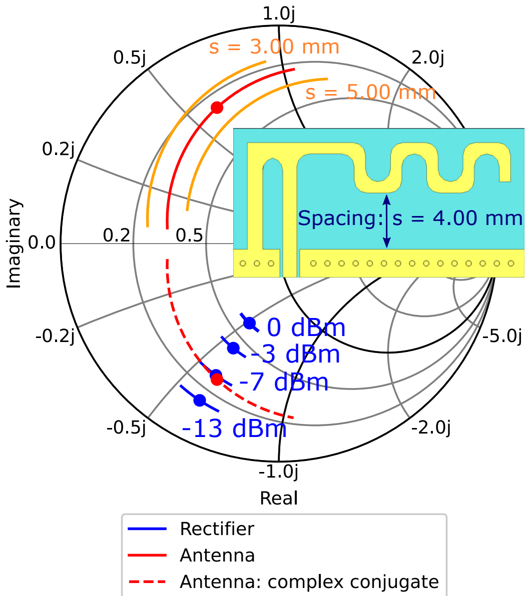

Fig. 3: Smith diagram with normalized input impedance from 2.35 to 2.55 GHz of the antenna and of the rectifier for an input power level of -13 dBm, -7 dBm, -3 dBm and 0 dBm.

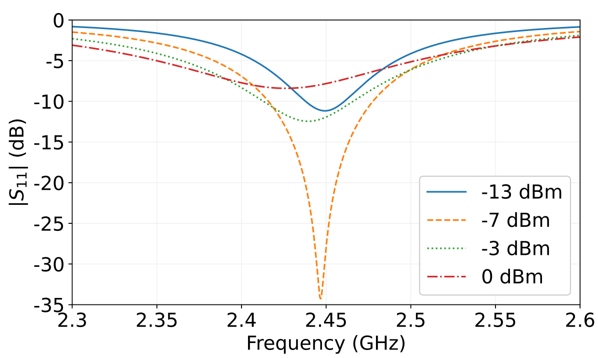

Fig. 4: Reflection coefficient $|S_{11}|$ [dB] versus frequency when conjugate-matched to the rectifier input impedance at an input power level of -13 dBm, -7 dBm, -3 dBm and 0 dBm.

A Kemet FC0H474ZFTBR32 supercapacitor [7] with a capacitance of 47 mF and a maximum operating voltage of 5.5 V is exploited as the primary energy storage element for the CPMS. The energy demand can be configured by adjusting the control parameters of the storage element through the threshold resistors. These include: V_{ovdis} as the voltage limit when the low-dropout regulator (LDO) is disabled, V_{chrdy} as the minimum voltage to enable the LDO and V_{ovch} as the maximum voltage on the storage element before disabling the boost converter. The complete rectenna system, along with all its sub-components, is illustrated in Fig. 5.

D. Results

The performance of the complete rectenna system is evaluated through over-the-air efficiency measurements. Therefore, a realistic WPT link is established using a power transmitting platform [8] capable of transmitting a 2.45 GHz signal. This

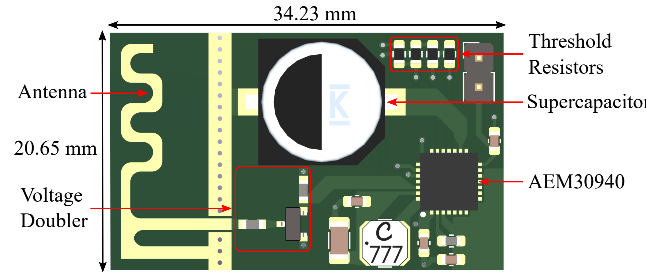

Fig. 5: Complete rectenna system.

transmitting platform is connected to an air-filled substrate integrated waveguide (AFSIW) cavity-backed slot antenna [9], with a gain of 6.02 dBi at the center frequency of 2.45 GHz. The distance between the rectenna system and the transmitting platform is set to 40 cm, which exceeds the upper limit of 29.79 cm for the radiating near field. The measurement setup for these over-the-air efficiency measurements is depicted in Fig. 6.

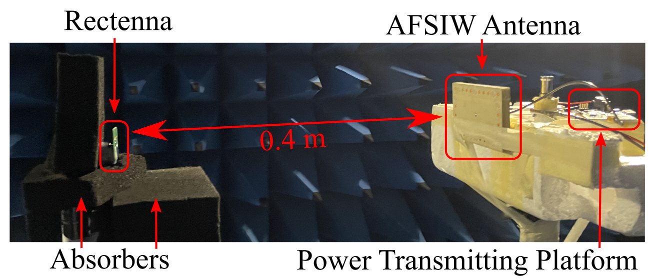

Fig. 6: Measurement setup for the over-the-air measurements.

To measure the over-the-air PCE of the rectenna, a prototype was assembled that included only the rectifier, excluding the CPMS. The output of the rectenna was connected to an optimal load resistance of 4.7 kΩ, as specified in [**?**]. The measured over-the-air PCE of the rectenna is presented in Fig. 7, alongside the simulated efficiency of the rectifier from [**?**]. For low input powers, ranging from -13 dBm to -1 dBm, the rectenna achieves PCEs that are equivalent to or even higher than the PCE of the rectifier when paired with a 50 Ω matching network.

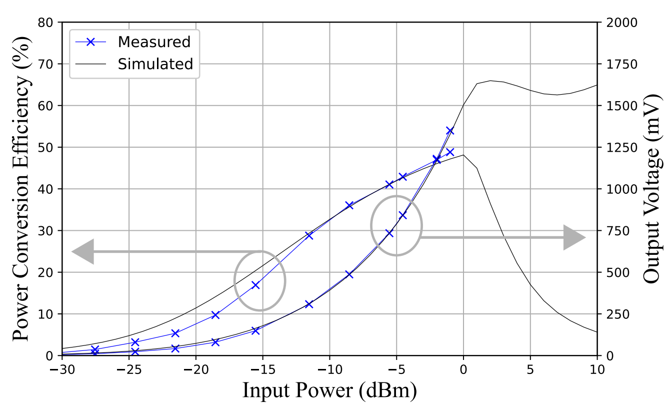

Fig. 7: PCE (%) and output voltage (mV), simulated and measured over-the-air as a function of input power (dBm) at 2.45 GHz.

E. Application

To demonstrate the functionality of the rectenna and the reconfigurable CPMS, an STM32WB55 ultra-low-power wireless microcontroller unit (MCU) USB Dongle was powered using the integrated LDO regulator output, providing 3.3 V. The application reads data from a MAX30102 body temperature sensor via an analog-to-digital converter (ADC) interface and transmits the sensor value using Bluetooth Low Energy (BLE) with a transmit power of 0 dBm. The transmission is optimized such that the data are encapsulated inside a BLE advertising packet to minimize the power consumption [10]. A single duty cycle, consisting of the start-up routine, data readout, and transmission of the advertising packet, consumes 10.76 mJ of energy when powered at 3.3 V and 7.78 mJ when powered at 1.8 V.

One of the default configurations for a dual-cell supercapacitor is V_{ovdis} = 3.60 V, V_{chrdy} = 3.92 V and V_{ovch} = 4.50 V. When this configuration is used with the 47 mF supercapacitor, the amount of energy that is available for the application amounts 56.55 mJ. The proposed application uses a lot less energy and therefore the threshold voltages are reconfigured. The following two examples use a different output voltage and a different threshold voltage configuration to demonstrate the reconfigurability. In each example the packet transmission rate was measured for different input power levels.

1) Example 1 - Output voltage of 3.3 V: The threshold voltages are configured to V_{ovdis} = 3.65 V and V_{chrdy} = 3.79 V via the threshold resistors for an output voltage of 3.3 V. This results in an available energy of 24.48 mJ, which is already closer to the actual needed energy but still a bit too high. The measured packet rate is averaged over 5 measurements and shown in Table I for different input power levels.

2) Example 2 - Output voltage of 1.8 V: Now, the threshold voltages are configured to V_{ovdis} = 2.34 V and V_{chrdy} = 2.25 V via the threshold resistors for an output voltage of 1.8 V. This results in an available energy of 9.71 mJ, which is more suited for the proposed application. The average packet update rate is shown again in Table I, showing a much higher update rate than in the first example. This highlights the importance of a well-configured CPMS when optimizing a real EH application.

TABLE I: Average packet update rate for both examples as a function of the input power level.

	Input Power Level	Average Update Rate
Example 1: 3.3 V 24.48 mJ	-1 dBm	110s (1m50s)
	-4 dBm	256s (4m16s)
	-7 dBm	817s (13m37s)
Example 2: 1.8 V 9.71 mJ	-1 dBm	26s
	-4 dBm	73s (1m13s)
	-7 dBm	372s (6m12s)
	-10 dBm	864s (14m24s)

III. Conclusion

The proposed rectenna system offers a promising solution for RF energy harvesting, with a focus on minimizing power losses and reducing system complexity. By co-designing and co-optimizing the antenna and rectifier, the rectenna achieves high efficiency, particularly at low input power levels typical of far-field WPT applications. The integration of a reconfigurable CPMS, featuring MPPT and a supercapacitor, ensures flexible and stable power delivery for low-power devices. Over-the-air efficiency measurements confirm that the rectenna system performs as well as, or better than, the rectifier with impedance matching networks. A practical demonstration involving the powering of an ultra-low-power MCU for BLE transmission further showcases the rectenna's applicability, featuring am average packet update rate of 14m24s for an input power level of -10 dBm, after optimizing the CPMS configuration. This work highlights the rectenna system's potential for enabling battery-free or battery-extended solutions in wireless sensing, RFID, and other low-power wireless applications.

Acknowledgement

This project was partially funded by the Flemish Research Foundation (FWO) SBO S001521N IoBaLeT (Sustainable Internet of Battery-Less Things) project and the FWO 3G0B9821 SafeHousePower project.

References

[1] K. Niotaki, N. B. Carvalho, A. Georgiadis, X. Gu, S. Hemour, K. Wu, D. Matos, D. Belo, R. Pereira, R. Figueiredo, H. Chaves, B. Mendes, R. Correia, A. Oliveira, V. Palazzi, F. Alimenti, P. Mezzanotte, L. Roselli, F. Benassi, A. Costanzo, D. Masotti, G. Paolini, A. Eid, J. Hester, M. M. Tentzeris, and N. Shinohara, "RF Energy Harvesting and Wireless Power Transfer for Energy Autonomous Wireless Devices and RFIDs," *IEEE Journal of Microwaves*, vol. 3, no. 2, pp. 763–782, 2023.

[2] B. Clerckx and A. Costanzo, "Toward 1G Mobile Power Networks," *IEEE Microwave Magazine*, vol. 19, no. August 2018, pp. 69–82, 2020.

[3] K. Gudan, S. Chemishkian, J. J. Hull, S. J. Thomas, J. Ensworth, and M. S. Reynolds, "A 2.4GHz ambient RF energy harvesting system with -20dBm minimum input power and NiMH battery storage," *2014 IEEE RFID Technology and Applications Conference, RFID-TA 2014*, pp. 7–12, 2014.

[4] G. Paolini, A. Quddious, D. Chatzichristodoulou, D. Masotti, S. Nikolaou, and A. Costanzo, "An Energy-Autonomous SWIPT RFID Tag for Communication in the 2.4 GHz ISM Band," *2022 3rd URSI Atlantic and Asia Pacific Radio Science Meeting, AT-AP-RASC 2022*, pp. 6–9, 2022.

[5] Skyworks, "SMS7630 Series," https://www.skyworksinc.com/Products/Diodes/SMS7630-Series, 2024.

[6] E-Peas, "AEM3040, Highly Efficient, Regulated Dual-Output, Ambient Energy Manager for AC or DC Sources with Optional Primary Battery." [Online]. Available: https://e-peas.com/wp-content/uploads/datasheets/ds-aem30940_qfn28-v1-6.pdf

[7] Kemet, "Supercapacitors FC Series." [Online]. Available: https://content.kemet.com/datasheets/KEM_S6011_FC.pdf

[8] J. Sennesael, J. Jocqué, T. Debuysscher, S. Lemey, J. Verhaevert, P. V. Torre, D. Schreurs, and H. Rogier, "Modular platform for efficient wireless power transfer to low-power devices," in *2024 4th URSI Atlantic Radio Science Meeting (AT-RASC)*, 2024, pp. 1–4.

[9] Q. Van Den Brande, S. Lemey, J. Vanfleteren, and H. Rogier, "Highly Efficient Impulse-Radio Ultra-Wideband Cavity-Backed Slot Antenna in Stacked Air-Filled Substrate Integrated Waveguide Technology," *IEEE Transactions on Antennas and Propagation*, vol. 66, no. 5, pp. 2199–2209, 2018.

[10] N. De Raeve, A. Shahid, M. De Schepper, E. De Poorter, I. Moerman, J. Verhaevert, P. Van Torre, and H. Rogier, "Bluetooth-Low-Energy-Based Fall Detection and Warning System for Elderly People in Nursing Homes," *Journal of Sensors*, vol. 2022, no. Ml, 2022.